Inverted hysteresis and giant exchange bias in $La_{0.7}Sr_{0.3}MnO_3/SrRuO_3$ superlattices

M. Ziese,[1,a)] I. Vrejoiu,[2] and D. Hesse[2]

[1]*Division of Superconductivity and Magnetism, University of Leipzig, 04103 Leipzig, Germany*
[2]*Max Planck Institute of Microstructure Physics, 06120 Halle, Germany*

The magnetization reversal mechanisms in a $La_{0.7}Sr_{0.3}MnO_3/SrRuO_3$ superlattice with ultrathin individual layers were studied. Due to the strong exchange bias between $La_{0.7}Sr_{0.3}MnO_3$ and $SrRuO_3$ layers inverted hysteresis loops were observed at temperatures below 62 K; at higher temperatures the superlattice showed an unconventional reversal mechanism with the magnetically hard $SrRuO_3$ layers switching first on reducing the magnetic field from saturation. These observations were corroborated by micromagnetic simulations and were interpreted as arising from interfacial Bloch walls. © *2010 American Institute of Physics*. [doi:10.1063/1.3470101]

Antiferromagnetic (AF) interlayer coupling and positive exchange bias were observed in $La_{0.7}Sr_{0.3}MnO_3$(LSMO)/ $SrRuO_3$ (SRO) bilayers and superlattices (SLs).[1–3] It was further shown that the AF interlayer coupling in LSMO/SRO SLs with ultrathin layers depended sensitively on interfacial intermixing and could be controlled using the intricate interplay between structure, magnetocrystalline anisotropy, magnitude of the layer magnetization, and layer thickness.[4] Here the magnetization reversal mechanisms in these SLs are shown to be unconventional which also affects the experimental determination of the exchange bias field. The latter is substantial in these samples.

A series of SLs was fabricated by pulsed laser deposition (KrF laser). Substrate temperature was 650 °C and oxygen partial pressure 0.14 mbar. Vicinal pure and Nb-doped $SrTiO_3$ (001) substrates with a miscut angle of about 0.1°, uniform TiO_2-termination and an atomically flat terrace morphology were used. The microstructure of the SLs was investigated by transmission electron microscopy (TEM), atomic force microscopy and x-ray diffractometry. A systematic study of the magnetic properties as a function of SRO layer thickness is published elsewhere.[4] Here we focus on the magnetic properties of a SL with LSMO layer thickness of 2.4 ± 0.4 nm and SRO layer thickness of 4.8 ± 0.4 nm grown on Nb:$SrTiO_3$. The magnetic properties of the SL were investigated by superconducting quantum interference device magnetometry. The magnetic moments were normalized to the LSMO volume only and were expressed in Bohr magneton per Mn ion. Micromagnetic simulations were performed with the Object Oriented MicroMagnetic Framework (OOMMF).[5]

Figure 1 shows two cross-sectional TEM images of the SL at different magnifications. Observations at various locations (not shown) revealed some extended lattice defects, e.g., dislocations—with the SL structure still existing close to these—that are presumably induced by defects and strain fields in the Nb:$SrTiO_3$ substrate. From the higher magnification TEM image the individual LSMO layer thickness was determined as 2.4 nm (6 unit cells), whereas the SRO layer thickness was about 4.8 nm. X-ray diffractometry in θ-2θ configuration showed satellite reflections up to the eighth

order around the (001) and (002) $SrTiO_3$ reflections. From these satellite peaks the SL period was determined as 7 ± 0.2 nm as well.

Figure 2 shows the field-cooled and remanent magnetization of the SL under various magnetic fields as a function of temperature. Magnetic fields were applied both parallel and perpendicular to the SL. Ferromagnetic order of the LSMO layers sets in at about 300 K and of the SRO layers at about 150 K. Below 150 K and in not too high fields the measured magnetic moment decreases with decreasing temperature indicating a strong AF interlayer coupling.[4] In higher fields, $\mu_0 H > 1$ T, the magnetization of the LSMO and SRO layers is gradually rotated toward the field direction. Since the remanent magnetization was significantly larger for in-plane than for perpendicular field, the data prove that the magnetic hard axis is along the SL normal. In the following we focus on in-plane magnetization measurements, since the magnetization processes in perpendicular fields are dominated by spin canting.

Magnetization hysteresis loops recorded at 10 and 100 K in in-plane magnetic fields are shown in Fig. 3. The most prominent feature of the hysteresis curves is the inversion of the central part of the loop at 10 K. Starting at high positive fields first the LSMO layers reverse their magnetization, but
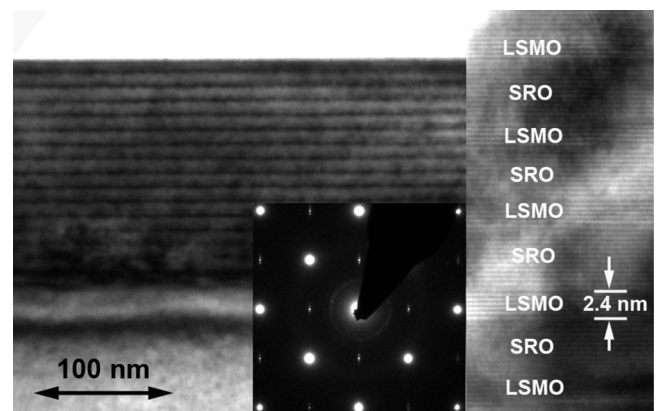

FIG. 1. Cross-sectional TEM images of the LSMO/SRO SL. Left: Overview TEM image of the entire thickness; right: (001) lattice plane image of part of the thickness. Inset: Diffraction pattern including SL reflections (tiny spots above and below weak main spots). Beam direction [100].

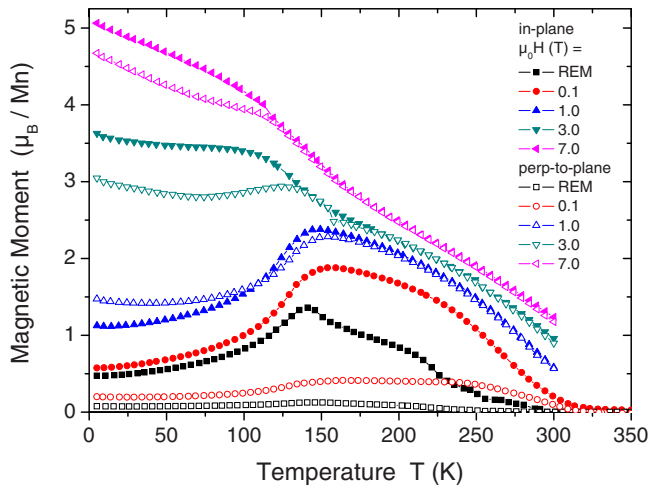a)Electronic mail: ziese@physik.uni-leipzig.de.

FIG. 2. (Color online) Magnetic moment per Mn ion measured in magnetic fields of 0.1, 1, 3, and 7 T applied parallel (solid symbols) and perpendicular (open symbols) to the SL. REM denotes the remanent magnetization measured after cooling the sample in 0.1 T to 5 K and removing the field.

still at positive fields, followed by the SRO layers at negative fields. Inverted ferromagnetic loops are rare;[6,7] the partially inverted loops observed here are thermodynamically allowed, since the work done in a full hysteresis cycle is positive. In contrast to the 10 K data the switching mechanism at 100 K proceeds along a different route as follows: the SRO layers reverse first at about ± 1.6 T, followed by a switching of the overall ferrimagnetic SL magnetization in low fields and a further switching of the SRO layers to a mainly parallel orientation at about ∓ 2.5 T. Between these two types of
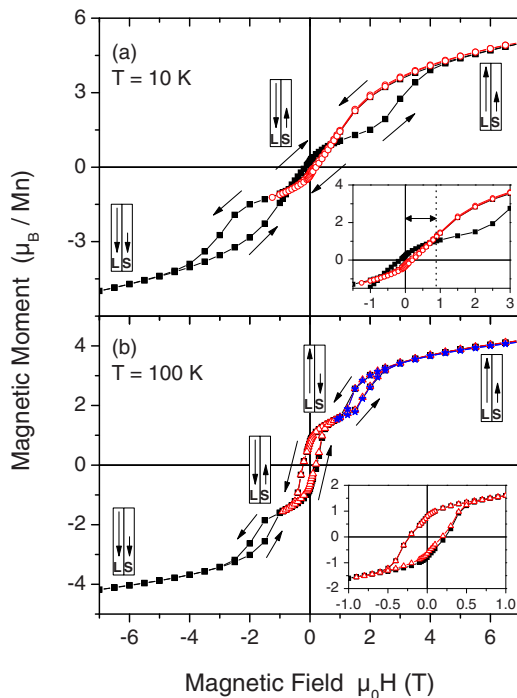

FIG. 3. (Color online) Full (solid symbols) and minor hysteresis loops at (a) 10 K and (b) 100 K. At 10 K one reversible minor loop is cycled between +7 T and −1.25 T, at 100 K two minor loops were measured, one (triangles) between +7 and −0.9 T and a second star between +7 and +0.9 T. The arrows indicate the sweep direction. The relative layer magnetization orientation is illustrated in the diagrams showing schematically a SL unit cell with a LSMO (L) and a SRO (S) layer. The insets show zooms of the central sections of the loops.

hysteresis loop, compensation is reached at a temperature of about 62 K with reversible low field magnetization behavior.

These hysteresis loops are exceptional for two following reasons: (i) at low temperatures the central hysteresis part is inverted, whereas the sequence of switching; magnetically soft LSMO layers reversing first, magnetically hard SRO layers reversing consecutively at fields of opposite polarity, is conventional; (ii) at higher temperatures the central hysteresis part is normal, but the magnetically hard layers reverse first, which is unconventional. These results can be understood as follows. The magnetic moments in bulk LSMO and SRO are about 3.7 μ_B/Mn and 1.6 μ_B/Ru, i.e., for this SL the layer magnetic moment of LSMO is larger than that of SRO. Accordingly, the layer magnetization state of this SL in zero field is ferrimagnetic. Bloch magnetic domain walls nucleated at the interfaces still persist to high magnetic fields leading to an exchange-spring state[8] and lack of saturation at 7 T due to spin canting. The magnetization reversal mechanism in this SL that has only six Mn spins across the LSMO layer thickness is determined by an interplay between magnetocrystalline anisotropy and the Bloch wall width.[9] At low temperatures the magnetocrystalline anisotropy of the SRO layers is large, such that on decreasing the magnetic field from its maximum absolute value the Bloch walls at the interfaces expand into the LSMO layers with these reversing first. At higher temperatures, however, the magnetocrystalline anisotropy in the SRO layers seems to be sufficiently weak, such that it is energetically more favorable for the Bloch walls to expand into the SRO layers and reverse the magnetization of these first; in intermediate fields the ferrimagnetic SL magnetization is then reversed leading to a three step hysteresis loop. This scenario is supported by the observation that in SLs with thinner LSMO layers (4 unit cells) only the second reversal mechanism is observed.[4] Moreover, single SRO films show a transition in the magnetocrystalline anisotropy between 60 and 70 K (Ref. 10) in agreement with the compensation temperature of 62 K observed here.

Micromagnetic simulations were carried out for SL stacks with five LSMO (1.6 nm or 2.4 nm)/SRO (4.8 nm) bilayers; in-plane size was 4×4 nm^2 with a cell size of 0.4 nm^3. Further parameters were exchange stiffnesses A of 5 pJ/m (LSMO) and 2 pJ/m (SRO), cubic magnetocrystalline anisotropy with $K_1 = -5$ kJ/m^3 (LSMO) and 500 kJ/m^3 (SRO) as well as a saturation magnetization of 0.74 T (LSMO) and 0.18 T (SRO). The AF interlayer exchange stiffness was varied between −0.05 and −3.2 pJ/m and the magnetic field was applied close to the [100] direction. The results of these simulations are only expected to yield qualitative insights, since SRO layers have orthorhombic and not cubic symmetry[10,11] and since the SL stack is always in the single domain regime. Keeping these caveats in mind, the simulations, see Fig. 4(a), showed that the influence of the LSMO layer thickness was negligible, whereas the interlayer exchange stiffness is a crucial parameter. For small AF coupling $A \geq -0.1$ pJ/m inverted hysteresis loops were obtained with the LSMO layers reversing first. For larger absolute values of the interlayer exchange stiffness $A \leq -0.4$ pJ/m a simultaneous coherent rotation of both LSMO and SRO layers occurs with an almost reversible hysteresis loop. This is a clear indication that the reversal mechanism proposed here is correct and is mainly controlled by the strength of the interfacial interlayer coupling.
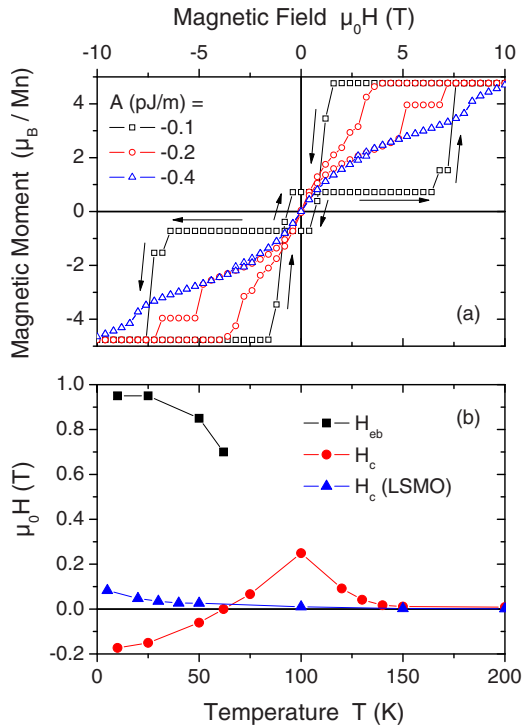
FIG. 4. (Color online) (a) Calculated magnetic hysteresis loops obtained from micromagnetic simulations for three values of the AF interlayer exchange stiffness. The arrows indicate the sweep direction. (b) Experimental exchange bias field H_{eb} and coercive fields H_c of the SL and a 5 nm thick single LSMO layer as a function of temperature.

Apart from the full hysteresis loops, Fig. 3 shows minor hysteresis loops recorded at 10 and 100 K. All hysteresis loops were measured after cooling from 200 K in +7 T. The minor loop measured at 10 K is clearly shifted vertically upward and to positive fields, see inset to Fig. 3(a), yielding a positive exchange bias field in agreement with earlier reports.[1,2] The exchange bias field H_{eb} was determined from the horizontal shift in the midpoint of the minor loop, see arrow and dashed line in the inset to Fig. 3(a). Above the compensation point of 62 K exchange bias is not clearly observed as illustrated in Fig. 3(b) and its inset; at 100 K neither the central loop nor the high field loop centered around 1.7 T are strongly shifted along the field axis. This does not imply that exchange biasing is absent; it just shows that the exchange bias field cannot be determined from hysteresis loops in which the magnetically hard layer switches first. Figure 4(b) shows the exchange bias field H_{eb} as a function of the temperature; the values of the exchange bias field are much larger than those found in Ref. 1 probably due to the much smaller thickness of the LSMO layers. Further the coercive fields H_c of the SL and a 5 nm thick LSMO single film are shown in Fig. 4(b). The coercive field of the SL changes sign at the compensation point of 62 K due to the hysteresis loop inversion below this temperature. Since the H_c values of the single film are smaller than those of the SL, one might conclude that the coercive field of the SL is mainly determined by the interfacial exchange coupling.

In summary, two different unconventional magnetization reversal mechanisms in a LSMO/SRO SL with ultrathin layers were observed. This was interpreted by the interplay of magnetocrystalline anisotropy energy, AF exchange coupling strength and interfacial Bloch wall width.

[1]X. Ke, M. S. Rzchowski, L. J. Belenky, and C. B. Eom, Appl. Phys. Lett. **84**, 5458 (2004).

[2]X. Ke, L. J. Belenky, C. B. Eom, and M. S. Rzchowski, J. Appl. Phys. **97**, 10K115 (2005).

[3]P. Padhan, W. Prellier, and R. C. Budhani, Appl. Phys. Lett. **88**, 192509 (2006).

[4]M. Ziese, I. Vrejoiu, E. Pippel, P. Esquinazi, D. Hesse, C. Etz, J. Henk, A. Ernst, I. V. Maznichenko, W. Hergert, and I. Mertig, Phys. Rev. Lett. **104**, 167203 (2010).

[5]M. J. Donahue and D. G. Porter, National Institute of Standards and Technology, Interagency Report No. NISTIR 6376, 1999 (unpublished).

[6]Y. Uozu, T. Nakajima, M. Nakamura, Y. Ogimoto, M. Izumi, and K. Miyano, Appl. Phys. Lett. **85**, 2875 (2004).

[7]J. Park, D. R. Lee, Y. Choi, J. W. Freeland, K. B. Lee, S. K. Sinha, K. R. Nikolaev, and A. M. Goldman, Appl. Phys. Lett. **95**, 102504 (2009).

[8]S. Mangin, G. Marchal, and B. Barbara, Phys. Rev. Lett. **82**, 4336 (1999).

[9]K. Dumesnil, C. Dufour, P. Mangin, A. Rogalev, and F. Wilhelm, J. Phys.: Condens. Matter **17**, L215 (2005).

[10]M. Ziese, I. Vrejoiu, and D. Hesse, Phys. Rev. B **81**, 184418 (2010).

[11]Q. Gan, R. A. Rao, C. B. Eom, L. Wu, and F. Tsui, J. Appl. Phys. **85**, 5297 (1999).